JOURNAL OF GUIDANCE, CONTROL, AND DYNAMICS
Vol. 34, No. 3, May–June 2011

Engineering Notes

Solution Based on Dynamical Approach for Multiple-Revolution Lambert Problem

P. V. Arlulkar* and S. D. Naik†
Defence Institute of Advanced Technology, Girinagar, Pune, Maharashtra 411 025, India,

DOI: 10.2514/1.51723

I. Introduction

THE classical Lambert problem deals with determination of the transfer velocity vector at an initial position to reach a final position in the specified time of flight. The multiple-revolution Lambert problem (MRLP) results when the interception takes place after completing one or more revolutions around the central body. In the case of the classical Lambert problem, the angular displacement between two positions is between 0 and 2π, while for the MRLP, it exceeds 2π. The total time of flight for the MRLP with N revolutions is the sum of N times the period of transfer orbit and the direct time of flight. There exists a total of $2N + 1$ solutions for N complete revolutions. A simple algorithm to solve the MRLP is of great interest for spacecraft interception, rendezvous, and interplanetary transfer. The MRLP approach allows a larger navigational flexibility and results in lower energy orbits than the direct transfer arcs.

A good amount of research has been made on the classical Lambert problem. Some of the approaches are extended for the MRLP solution as well as optimization for fuel or velocity. The solution for the classical Lambert problem was first attempted by Gauss [1]. The universal variable formulation method was applied for solving the classical Lambert problem as well as the MRLP in Bate et al. [2]. Battin and Vaughan [3] attempted the classical Lambert problem with the semimajor axis as an independent parameter and solved it with the help of the hypergeometric series. Separate algorithms for the high and low energy transfers to the MRLP with the Battin and Vaughan formulation were evolved by Loechler [4]. Prussing [5] used the Lagrange formulation for the minimum-fuel multiple-revolution algorithm for an elliptic orbit to determine all the possible transfer trajectories. Shen and Tsiotras [6] extended it for the minimum velocity fixed-time two-impulse transfer algorithm between two coplanar circular orbits. The transverse eccentricity vector-based algorithm was given by Avanzini [7]. He et al. [8] extended Avanzini's [7] approach for the MRLP and improved the convergence of the algorithm. All these approaches used the Kepler time equation for calculating the time of flight. A dynamical approach has been developed by Nelson and Zarchan [9] for solving the classical Lambert problem. It is based on the closed-form solution of the equations of motion given by Wheelon [10]. Velocity and time of flight are obtained as a function of flight-path angle as an independent parameter. The iterating variable (flight-path angle) and the terminating condition (time of flight) are physical parameters of the transfer orbit [9].

In this Note, we report a novel algorithm based on the dynamical approach for solving the MRLP with the flight-path angle as an independent parameter. The expression for the total time of flight is obtained. The high and low energy orbits get separated using a derivative of total time of flight with respect to the flight-path angle. The algorithm is fast and easy to understand. It is noteworthy that the results obtained are in complete agreement with He et al. [8].

II. Dynamical Approach

Consider a spacecraft with the initial position $\boldsymbol{r}_1$ and the final position $\boldsymbol{r}_2$; $t_{f\text{des}}$ defines the desired time of flight. Let θ_f be the transfer angle between $\boldsymbol{r}_1$ and $\boldsymbol{r}_2$ and $\boldsymbol{V}$ be the transfer velocity vector. Flight-path angle γ is the angle between the local horizontal direction and the velocity vector $\boldsymbol{V}$, as shown in the Fig. 1. The vector form of the equation of motion of a point mass in a uniform gravitational field is

$$\ddot{\mathbf{r}} = -\frac{\mu}{r^3}\mathbf{r} \tag{1}$$

Separating radial and transverse components, we get

$$\ddot{r} - r(\dot{\theta})^2 + \frac{\mu}{r^2} = 0 \tag{2}$$

$$r^2\dot{\theta} = r_1 V \cos\gamma \tag{3}$$

where the scalar is the norm of vector.

Solving these two equations simultaneously [9], the position as a function of angular displacement θ is

$$r(\theta) = \frac{r_1 \lambda \cos^2\gamma}{1 - \cos\theta + \lambda\cos\gamma\cos(\theta+\gamma)} \tag{4}$$

where

$$\lambda = r_1 V^2/\mu \tag{5}$$

Initial transfer velocity V at initial position as a function of the flight-path angle is obtained from Eqs. (4) and (5) for $\theta = \theta_f$ and $r(\theta) = r_2$:

$$V = \sqrt{\frac{\mu r_2(1-\cos\theta_f)}{r_1[r_1\cos^2\gamma - r_2\cos(\theta_f+\gamma)\cos\gamma]}} \tag{6}$$

where

$$\theta_f = \mathrm{mod}\left(a\tan 2\left\{\frac{\det[\mathbf{r_1 r_2}]^T}{\mathbf{r_1}\cdot\mathbf{r_2}}\right\}, 2\pi\right) \tag{7}$$

The time of flight for the direct transfer in elliptical orbit is obtained by substituting the value of r from Eq. (4) in Eq. (3) and integrating

$$t_f = \frac{r_1}{V\cos\gamma}\left\{\frac{\tan\gamma(1-\cos\theta_f) + (1-\lambda)\sin\theta_f}{(2-\lambda)\{(1-\cos\theta_f)/(\lambda\cos^2\gamma) + [\cos(\theta_f+\gamma)]/\cos\gamma\}} + \frac{2\cos\gamma}{\lambda[(2/\lambda)-1]^{1.5}}\tan^{-1}\left(\frac{\sqrt{2/\lambda - 1}}{\cos\gamma\cot(\theta_f/2) - \sin\gamma}\right)\right\} \tag{8}$$

Received 22 July 2010; revision received 7 January 2011; accepted for publication 8 January 2011.

*Senior Research Fellow, Department of Applied Mathematics; pvarlulkar@gmail.com.
†Scientist 'F', Department of Applied Mathematics; sdnaik@diat.ac.in.

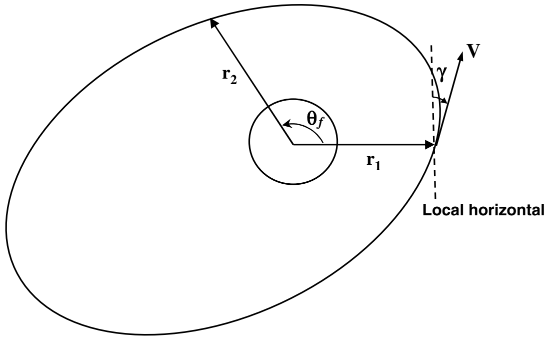

Fig. 1 Geometry of transfer orbit.

For elliptical orbits. the limits on the flight-path angle γ are

$$\gamma = \tan^{-1}\left[\frac{\sin\theta_f \pm \sqrt{(2r_1/r_2)(1-\cos\theta_f)}}{(1-\cos\theta_f)}\right] \tag{9}$$

The two limits are denoted by $\gamma_{\max}$ and $\gamma_{\min}$, respectively.

III. Extension to Multiple-Revolution Lambert Problem

In the direct transfer case, the spacecraft follows an arc between $\boldsymbol{r}_1$ to $\boldsymbol{r}_2$, whereas for multiple-revolution transfers, it completes one or more revolutions before the interception. The total time of flight for N revolutions is expressed in terms of orbit period t_p and direct transfer time of flight t_f from $\boldsymbol{r}_1$ to $\boldsymbol{r}_2$ as

$$T_f = Nt_p + t_f \tag{10}$$

The period of orbit by the Kepler third law of planetary motion is

$$t_p = 2\pi\sqrt{\frac{a^3}{\mu}} \tag{11}$$

where a is the semimajor axis of the transfer ellipse:

$$a = \frac{h^2/\mu}{1-e^2} \tag{12}$$

Substituting for $h = r_1 V\cos\gamma$ and $e^2 = 1 + \lambda(\lambda-2)\cos^2\gamma$, we get

$$a = \frac{r_1}{2-\lambda} \tag{13}$$

Equation (11) is converted to

$$t_p = \frac{2\pi}{\sqrt{\mu}}\left[\frac{r_1}{2-\lambda}\right]^{3/2} \tag{14}$$

Using Eqs. (5) and (6), t_p is expressed as a function of the flight-path angle. Substituting from Eqs. (8) and (14), Eq. (10) becomes

$$T_f = N\frac{2\pi}{\sqrt{\mu}}\left[\frac{r_1}{2-\lambda}\right]^{3/2} + \frac{r_1}{V\cos\gamma}\left\{\frac{\tan\gamma(1-\cos\theta_f)+(1-\lambda)\sin\theta_f}{(2-\lambda)\{(1-\cos\theta_f)/(\lambda\cos^2\gamma)+[\cos(\theta_f+\gamma)]/\cos\gamma\}} + \frac{2\cos\gamma}{\lambda[(2/\lambda)-1]^{1.5}}\tan^{-1}\left(\frac{\sqrt{(2/\lambda)-1}}{\cos\gamma\cot(\theta_f/2)-\sin\gamma}\right)\right\} \tag{15}$$

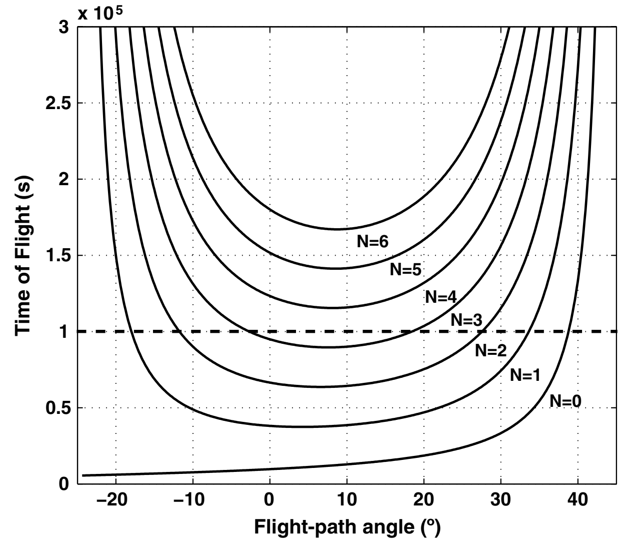

Fig. 2 Time of flight vs flight-path angle.

The total time of flight as a function of flight-path angle for the multiple revolution for N number of revolutions is plotted in Fig. 2. Here, $r_1 = 2R_E$ and $r_2 = 4R_E$, where R_E is the Earth radius and $\theta_f = 150°$. For the direct transfer ($N = 0$), the time of flight is monotonically increasing with the flight-path angle, as stated by Nelson and Zarchan [9]. For the multiple revolutions ($N \geq 1$), in the desired time of flight, there are two different flight-path angles corresponding to the high and low energy orbits. A single solution is possible only when $\mathrm{d}T_f/\mathrm{d}\gamma$ equals zero, corresponding to the minimum time of flight. The flight-path angle corresponding to the minimum time of flight is denoted by $\gamma_{t\min}$. For a desired time of flight of 1×10^5 s, there exists a total of seven solutions, as shown in Fig. 2. The direct transfer takes place at a flight-path angle equal to 38.8°. For multiple revolutions ($1 \leq N \leq 3$), high energy orbits having negative flight-path angles and low energy orbits have positive flight-path angles. The magnitude of the flight-path angle decreases as the number of revolutions increases. For $N = 4$, the minimum time of flight (1.155×10^5 s) is greater than the desired time of flight (1×10^5 s). Hence, no solution exists for $N \geq 4$.

IV. Approach for Multiple Revolution

The numerical procedure for finding all the solutions corresponding to the desired time of flight $t_{f\mathrm{des}}$ for the MRLP is described in this section. For given $\boldsymbol{r}_1$ and $\boldsymbol{r}_2$, the transfer angle θ_f is obtained from Eq. (7). The bounds on flight-path angle, $\gamma_{\min}$ and $\gamma_{\max}$, are calculated by Eq. (9). The initial guess is selected as the average value of these bounds of γ. The velocity and time of flight are calculated using Eqs. (6) and (15), respectively, as functions of γ. If the calculated time of flight is not equal to the desired time of flight, correct up to eight significant digits, the new flight-path angle is obtained by the secant method [9]. The iterative formula for new γ is given as

$$\gamma_{n+1} = \gamma_n + \frac{(\gamma_n-\gamma_{n-1})(t_{f\mathrm{des}}-T_n)}{(T_n-T_{n-1})} \tag{16}$$

For $N = 0$, $\gamma_0 = (\gamma_{\min}+\gamma_{\max})/2$. For $N \geq 1$, there exist two orbits for each value of N, which are separated by the minimum time of flight, which can be obtained mathematically by equating the first-order derivative of the time of flight to zero. The derivative of the time of flight with respect to the flight-path angle is given by

$$\frac{\mathrm{d}T_f}{\mathrm{d}\gamma} = N\frac{\mathrm{d}t_p}{\mathrm{d}\gamma} + \frac{\mathrm{d}t_f}{\mathrm{d}\gamma} \tag{17}$$

$$
\begin{aligned}
\frac{\mathrm{d}T_f}{\mathrm{d}\gamma} &= N\frac{3\pi r_1^{3/2}}{\sqrt{\mu}(2-\lambda)^{5/2}}\frac{\mathrm{d}\lambda}{\mathrm{d}\gamma} \\
&+ \frac{r_1}{V\cos\gamma}\left\{\frac{r_2}{r_1(2-\lambda)^2}\left[(2-\lambda)\left\{(1-\cos\theta_f)\sec^2\gamma-\sin\theta_f\frac{\mathrm{d}\lambda}{\mathrm{d}\gamma}\right\}\right.\right. \\
&\left.+\{\tan\gamma(1-\cos\theta_f)+(1-\lambda)\sin\theta_f\}\frac{\mathrm{d}\lambda}{\mathrm{d}\gamma}\right]+\left[\frac{2\cos\gamma}{\lambda[(2/\lambda)-1]^{3/2}}\right] \\
&\times\left[\frac{1}{[\cos\gamma\cot(\theta_f/2)-\sin\gamma]^2+(2/\lambda)-1}\right] \\
&\times\left[\frac{\cos\gamma\cot(\theta_f/2)-\sin\gamma}{2[(2/\lambda)-1]^{1/2}\lambda^2}\frac{\mathrm{d}\lambda}{\mathrm{d}\gamma}+\left(\frac{2}{\lambda}-1\right)^{1/2}\left(\sin\gamma\cot\frac{\theta_f}{2}+\cos\gamma\right)\right] \\
&-\tan^{-1}\left(\frac{\sqrt{(2/\lambda)-1}}{\cos\gamma\cot(\theta_f/2)-\sin\gamma}\right)\times\left[\frac{2}{\lambda[(2/\lambda)-1]^{3/2}}\right] \\
&\left.\times\left[\sin\gamma+\frac{\cos\gamma}{2\lambda}\frac{\mathrm{d}\lambda}{\mathrm{d}\gamma}\left(\frac{1+2\lambda}{2-\lambda}\right)\right]\right\}-\frac{r_1}{V^2\cos^2\gamma} \\
&\times\left\{\frac{\tan\gamma(1-\cos\theta_f)+(1-\lambda)\sin\theta_f}{(2-\lambda)([(1-\cos\theta_f)/(\lambda\cos^2\gamma)]+\{[\cos(\theta_f+\gamma)]/\cos\gamma\})}\right. \\
&\left.+\frac{2\cos\gamma}{\lambda[(2/\lambda)-1]^{1.5}}\tan^{-1}\left(\frac{\sqrt{(2/\lambda)-1}}{\cos\gamma\cot(\theta_f/2)-\sin\gamma}\right)\right\} \\
&\times\left[\frac{\mathrm{d}V}{\mathrm{d}\gamma}\cos\gamma-V\sin\gamma\right]
\end{aligned}
\tag{18}
$$

where

$$\frac{\mathrm{d}\lambda}{\mathrm{d}\gamma}=\lambda\left[\frac{-r_2\sin(\theta_f+2\gamma)+r_1\sin\gamma}{r_1\cos^2\gamma-r_2\cos(\theta_f+\gamma)\cos\gamma}\right]$$

$$\frac{\mathrm{d}V}{\mathrm{d}\gamma}=\frac{V}{2}\left[\frac{-r_2\sin(\theta_f+2\gamma)+r_1\sin\gamma}{r_1\cos^2\gamma-r_2\cos(\theta_f+\gamma)\cos\gamma}\right]$$

Equating Eq. (18) to zero and solving for γ gives $\gamma_{t\min}$. The initial transfer velocity at r_1, corresponding to the minimum time of flight, is denoted by $V_{t\min}$. This leads to an algorithm for the solution of the MRLP for the given boundary conditions. The limits on the flight-path angle and $\gamma_{t\min}$ are plotted in Fig. 3. Here, the boundary conditions are $r_1 = 2R_E$, $r_2 = 4R_E$, and $N = 2$. The flight-path angle corresponding to the minimum time of flight monotonically decreases with the transfer angle. The interval for γ is selected for the high energy transfer orbit as $\gamma_{\min} < \gamma < \gamma_{t\min}$ and for the low energy transfer as $\gamma_{t\min} < \gamma < \gamma_{\max}$. It is observed that $V_{t\min}$ is the maximum for the central angle equal to 180°.

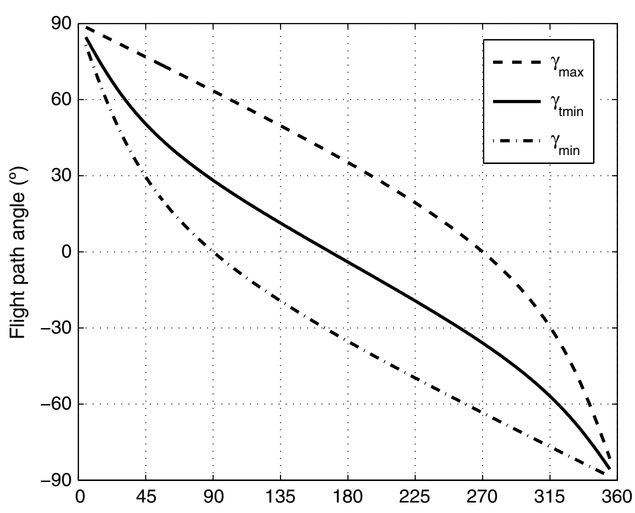

Fig. 3 Flight-path angle vs transfer angle.

Table 1 Case studies

Case	r_1, Earth radius	r_2, Earth radius	θ_f, °	$N_{\max}$	Iteration range
I	2	3	150	4	9–12
II	2	4	150	3	6–9
III	2	4	220	3	6–9
IV	2	7	220	1	8–10

An algorithm for all solutions of the MRLP is developed by the dynamical approach. The steps involved are as follows:

1) Input $\boldsymbol{r}_1$ and $\boldsymbol{r}_2$ in the orbital plane and $t_{f\mathrm{des}}$.
2) Calculate the θ_f from Eq. (7).
3) Calculate the limits on the flight-path angle, $\gamma_{\min}$ and $\gamma_{\max}$, for elliptical orbits from Eq. (9).
4) Iterate on γ to find the solution for the direct transfer with $N = 0$.
5) For $N = N + 1$, find out $\gamma_{t\min}$ for the minimum time of flight by equating $\mathrm{d}T_f/\mathrm{d}\gamma$ [Eq. (18)] to zero.
6) For the high energy transfer orbit, replace $\gamma_{\max}$ by $\gamma_{t\min}$ and iterate.
7) For the low energy transfer orbit, replace $\gamma_{\min}$ by $\gamma_{t\min}$ and iterate.
8) Continue steps 5 to 7 until the minimum time of flight for the Nth revolution is less than $t_{f\mathrm{des}}$.
9) The maximum number of allowed revolutions is $N_{\max} = N - 1$.

V. Simulation Study

To check the performance of the algorithm, four cases are studied, which are summarized in Table 1. In these cases, r_1 and r_2 are greater than the Earth radius, and the transfer angle θ_f is selected from the second and third quadrants. The desired time of flight $t_{f\mathrm{des}}$ is 1×10^5 s. The last two columns in Table 1 show the maximum number of allowed revolutions $N_{\max}$ and the range of iteration required to solve the problem.

The computation time required for the algorithm given in this Note for a case study on a 2.66 GHz, 2 GB RAM personal computer is around 35 μs.

Figure 4 shows the initial transfer velocity corresponding to the number of revolutions for case I. The direct transfer velocity corresponds to $N = 0$. Low energy transfer velocities and high energy transfer velocities decrease monotonically with the number of revolutions. The initial transfer velocity is the minimum for the low energy orbit of the maximum allowed revolution. Similar results are also obtained for cases II, III, and IV.

The effect of central angle for the desired time of flight for fixed r_1 and r_2 has been studied in Fig. 5. The data used are $r_1 = 2R_E$ and

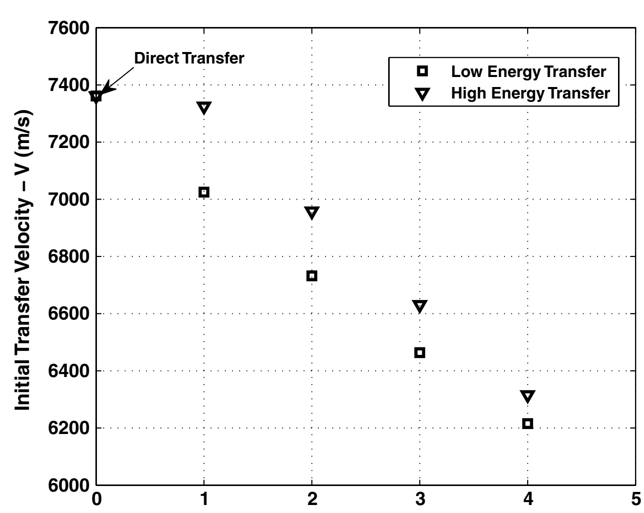

Fig. 4 Transfer velocity vs number of revolutions.

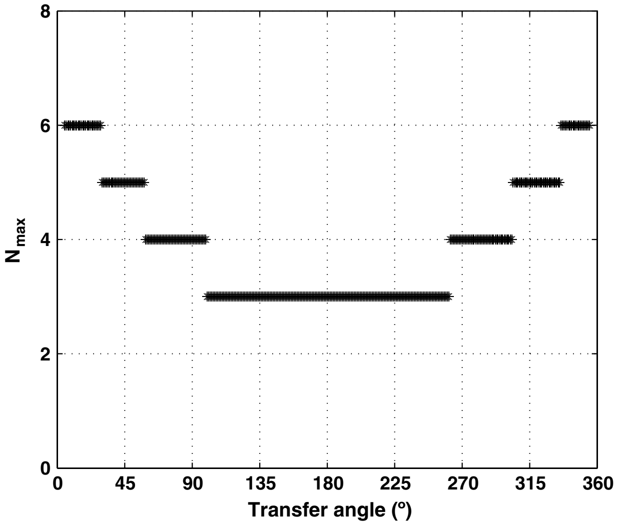

Fig. 5 $N_{\max}$ for different transfer angles.

$r_2 = 4R_E$, and the desired time of flight equals 1×10^5 s for $\theta = 5$–$355°$. The minimum number of $N_{\max}$ occurs for the central angle at 180° and extends over the equal intervals on both the sides. $N_{\max}$ decreases in the first and second quadrants, whereas it increases in the third and fourth quadrants with the central angle. From Fig. 5, the minimum value of $N_{\max}$ is three, which is observed over an interval of 100–260°. The minimum number of $N_{\max}$ is increased as the desired time of flight increases.

The results obtained by the approach are in complete agreement with the approach given by He et al. [8].

VI. Conclusions

A simple algorithm is developed for the MRLP using the dynamical approach based on the flight-path angle. The dynamical approach is obtained from closed-form solutions of the equations of motion and requires no knowledge of the geometry of the conic section. The algorithm is easy to understand. The derivative of the total time of flight separates the low and the high energy transfer orbits. The algorithm gives orbit specification in terms of flight-path angle, which is a physical parameter for all the allowed revolutions.

Acknowledgments

The authors are thankful to the Vice Chancellor of the Defence Institute of Advanced Technology (DIAT), Girinagar (India), for granting permission to publish this work. The authors are also thankful to R. S. Deodhar of the Department of Applied Mathematics, DIAT (India) for fruitful discussions.

References

[1] Gauss, K. F., “Theory of Motion of the Heavenly Bodies Moving About the Sun in Conic Sections,” Dover, New York, 1963.

[2] Bate, R. R., Mueller, D. D., and White, J. E., *Fundamentals of Astrodynamics*, Dover, New York, 1971, pp. 227–276.

[3] Battin, R. H., and Vaughan, R. M., “An Elegant Lambert Algorithm,” *Journal of Guidance, Control, and Dynamics*, Vol. 7, No. 6, 1984, pp. 662–670.
doi:10.2514/3.19910

[4] Loechler, L. A., “An Elegant Lambert Algorithm for Multiple Revolution Orbits,” M.S. Thesis, Department of Aeronautics and Astronautics, Massachusetts Inst. of Technology, Cambridge, MA, 1988.

[5] Prussing, J. E., “A Class of Optimal Two-Impulse Rendezvous Using Multiple-Revolution Lambert Solutions,” *Journal of the Astronautical Sciences*, Vol. 48, No. 2, April–Sept. 2000, pp. 131–148; alsoalso American Astronautical Society Paper AAS 00-250 Springfield, VA, 2000.

[6] Shen, H. J., and Tsiotras, P., “Optimal Two-Impulse Rendezvous Using Multiple-Revolution Lambert Solutions,” *Journal of Guidance, Control, and Dynamics*, Vol. 26, No. 1, 2003, pp. 50–61.
doi:10.2514/2.5014

[7] Avanzini, G., “A Simple Lambert’s Algorithm,” *Journal of Guidance, Control, and Dynamics*, Vol. 31, No. 6, 2008, pp. 1587–1594.
doi:10.2514/1.36426

[8] He, Q., Li, J., and Han, C., “Multiple Revolution Solution of the Transverse Eccentricity Based Lambert Problem,” *Journal of Guidance, Control, and Dynamics*, Vol. 33, No. 1, 2010, pp. 265–268.
doi:10.2514/1.45041

[9] Nelson, S. L., and Zarchan, P., “Alternative Approach to the Solution of Lambert’s Problem,” *Journal of Guidance, Control, and Dynamics*, Vol. 15, No. 4, 1992, pp. 1003–1009.
doi:10.2514/3.20935

[10] Wheelon, A. D., “Free Flight of a Ballistic Missile,” *ARS Journal*, Vol. 29, No. 12, 1959, pp. 915–926.